

Mouse Embryonic Head as a Site for Hematopoietic Stem Cell Development

Zhuan Li,^{1,2,11} Yu Lan,^{3,11} Wenyan He,¹ Dongbo Chen,¹ Jun Wang,³ Fan Zhou,¹ Yu Wang,³ Huayan Sun,¹ Xianda Chen,¹ Chunhong Xu,¹ Sha Li,¹ Yakun Pang,⁴ Guangzhou Zhang,⁵ Liping Yang,⁵ Lingling Zhu,⁶ Ming Fan,⁶ Aijia Shang,⁷ Zhenyu Ju,⁸ Lingfei Luo,² Yuqiang Ding,⁹ Wei Guo,¹⁰ Weiping Yuan,⁴ Xiao Yang,^{3,*} and Bing Liu^{1,2,4,*}

¹307-Ivy Translational Medicine Center, Laboratory of Oncology, Affiliated Hospital of Academy of Military Medical Sciences, Beijing 100071, China

²Key Laboratory of Freshwater Fish Reproduction and Development, Ministry of Education, Laboratory of Molecular Developmental Biology, School of Life Science, Southwest University, Chongqing 400715, China

³State Key Laboratory of Proteomics, Genetic Laboratory of Development and Diseases, Institute of Biotechnology, Beijing 100071, China

⁴State Key Laboratory of Experimental Hematology, Institute of Hematology and Blood Diseases Hospital, Chinese Academy of Medical Sciences, Tianjin 300020, China

⁵Laboratory Animal Center of Academy of Military Medical Sciences, Beijing 100071, China

⁶Department of Brain Protection and Plasticity, Institute of Basic Medical Sciences, Beijing 100850, China

⁷Department of Neurosurgery, General Hospital of Chinese PLA, Beijing 100853, China

⁸Max-Planck-Partner Group on Stem Cell Aging, Institute of Aging Research, College of Medicine Hangzhou Normal University, Zhejiang 310036, China

⁹Key Laboratory of Arrhythmias, Ministry of Education, East Hospital, Tongji University School of Medicine, Shanghai 200092, China

¹⁰Center for Stem Cell Biology and Regenerative Medicine, School of Medicine, Tsinghua University, Beijing 100084, China

¹¹These authors contributed equally to this work

*Correspondence: yangx@nic.bmi.ac.cn (X.Y.), bingliu17@yahoo.com (B.L.)

<http://dx.doi.org/10.1016/j.stem.2012.07.004>

SUMMARY

In the mouse embryo, the aorta-gonad-mesonephros (AGM) region is considered to be the sole location for intraembryonic emergence of hematopoietic stem cells (HSCs). Here we report that, in parallel to the AGM region, the E10.5–E11.5 mouse head harbors bona fide HSCs, as defined by long-term, high-level, multilineage reconstitution and self-renewal capacity in adult recipients, before HSCs enter the circulation. The presence of hemogenesis in the midgestation head is indicated by the appearance of intravascular cluster cells and the blood-forming capacity of a sorted endothelial cell population. In addition, lineage tracing via an inducible *VE-cadherin-Cre* transgene demonstrates the hemogenic capacity of head endothelium. Most importantly, a spatially restricted lineage labeling system reveals the physiological contribution of cerebrovascular endothelium to postnatal HSCs and multilineage hematopoiesis. We conclude that the mouse embryonic head is a previously unappreciated site for HSC emergence within the developing embryo.

INTRODUCTION

Hematopoietic stem cells (HSCs) can continuously produce hematopoietic cells of all lineages throughout the lifetime of an individual. Experimentally, they are defined by the competence

to engraft into the bone marrow (BM) of lethally irradiated recipients and the ability to rebuild all the components of hematopoietic system via self-renewal and differentiation. Whereas BM serves as the main niche for supporting HSC activity in postnatal stage, the early emergence, stepwise maturation, and remarkable expansion of fetal HSCs occurs in different locations and is temporally restricted during mouse embryogenesis (Cumano and Godin, 2007; Dzierzak and Speck, 2008; Mikkola and Orkin, 2006).

The first visible blood cells, the nucleated primitive erythrocytes producing embryonic hemoglobin, arise in the mouse extraembryonic yolk sac (YS) at embryonic day 7.0–7.5 (E7.0–7.5), concomitant with the developing vasculature (McGrath and Palis, 2005). Shortly thereafter, the YS yields a cohort of unilineage and multilineage erythromyeloid progenitors that can migrate into the embryo proper via circulation (Lux et al., 2008). As the HSCs are positioned at the top of the hematopoietic hierarchy and can ensure life-long production of blood cells, the questions of when, where, and how the HSCs are generated during mammalian embryogenesis are under intensive investigations but remain highly debated (Yoshimoto et al., 2008). Among various midgestation embryonic tissues, the cells capable of long-term, high-level, and multilineage hematopoietic repopulation can first be exclusively detected in the E10.5 (>35 somite pairs; sp) aorta-gonad-mesonephros (AGM) region (Müller et al., 1994). As further revealed by organ or reaggregation cultures, the HSC potential of the AGM region can be autonomously and remarkably augmented via maturation of a large number of nascent HSC precursors (pre-HSCs) (Cumano et al., 1996; Medvinsky and Dzierzak, 1996; Taoudi et al., 2008). Moreover, HSCs are detected simultaneously or slightly later in other major vessels (umbilical arteries and vitelline arteries) or highly vascularized structures (placenta and YS) at E10.5–E11.0

(de Bruijn et al., 2000; Gekas et al., 2005; Ottersbach and Dzierzak, 2005; Rhodes et al., 2008). Interestingly, a type of newborn-repopulating HSC has been identified in both the YS and the para-aortic splanchnopleura (P-Sp, destined to form the AGM region) of E9.5 embryos via intraliver transplantation. Such cells are CD34⁺c-Kit⁺ and CD41⁺, and can further engraft into the BM of adults, implicating that they are immature precursors of adult-type HSCs (Ferkowicz et al., 2003; Yoder et al., 1997). Furthermore, using a nonheartbeat *Ncx1*^{-/-} mouse model, T and B lymphoid potential are observed in the P-Sp, YS, and placenta of E9.5 embryos, suggesting that the generation of lymphoid progenitor cells is independent of circulation (Rhodes et al., 2008). Notably, the placenta contains 15-fold more HSCs than AGM and YS at E12.5–E13.5 (Gekas et al., 2005). Unlike the hemogenic sites, the fetal liver cannot form HSCs de novo but is colonized by external HSCs via circulation (Zovein et al., 2008).

During the entire course of embryonic hematopoiesis, the formation of blood cells is closely correlated with vascular development. For the mouse embryo proper, vasculogenesis is initiated at E7.3 in the cranial part, and the dorsal aorta becomes discernable slightly later (Drake and Fleming, 2000). Interestingly, putative angioblasts within the rostral vasculature coexpress Flk-1 and Scl, the markers of hematopoietic specification from mesodermal precursors. By analyzing the hemogenic potential of epiblast tissue at E6.5–E7.7, Kanatsu et al. found that the anterior head-fold has hemogenic potential if activin or BMP4 is added (Kanatsu and Nishikawa, 1996). At E9.5, the head contains a number of erythromyeloid progenitors no less than the number in the AGM region (Palis et al., 1999). More strikingly, after the AGM and fetal liver are removed, the remnants of the E11 embryo proper demonstrate robust HSC potential in vivo, which is not detected in concomitant circulating cells (Müller et al., 1994). Intriguingly, prior to circulation, the zebrafish head is an important site for early embryonic hematopoiesis, including genesis of macrophages and granulocytes (Bennett et al., 2001; Herbolme et al., 1999; Le Guyader et al., 2008). The above direct and indirect clues prompted us to comprehensively analyze the hematopoietic activity in the rostral half of embryo proper during mouse midgestation.

Here, we report that the mouse E10.5–E11.5 head harbors authentic HSCs, which demonstrate long-term, efficient, and multilineage reconstitution and self-renewal capacity in lethally irradiated adult recipients. Such potential cannot be explained by later and rare emergence of HSCs in the embryonic circulation. Development of hemogenic endothelium in the head is further confirmed by morphological, functional, and lineage tracing strategies. More convincingly, in a unique *SP-A-Cre* transgenic mouse model, which is a fully physiological setting, the cerebrovascular endothelium demonstrates de novo hematopoietic potential and contribution to postnatal HSCs.

RESULTS

Erythromyeloid Progenitors in the Mouse Embryonic Head

In E9.5–E12.5 embryos (Figure 1A, a representative E10.5 embryo), the numbers of colony-forming units in the culture (CFU-Cs) of the caudal half (CH) or AGM region seemed steady

(Figure 1B). In contrast, dramatic changes were observed in the head region. The number of CFU-Cs was increased from E9.5 (131 per tissue), peaked at E11.5 (1,074 per tissue), and then declined at E12.5 (704 per tissue). The percentage of CFU-GM and CFU-Mix in the head and CH/AGM appeared to be comparable between E9.5–E11.5 (Figure 1C, and data not shown). The CFU-Cs in the E10.5–11.0 head were mainly enriched in the Tie2⁺ population (Figure 1D).

B and T Lymphoid Potential in the Mouse Embryonic Head

Lymphoid potential is thought to be an important indicator of definitive hematopoiesis. Here, the OP9 and OP9-DL1 cells were used to induce B and T lymphocytes, respectively. After being cocultured with the OP9 cells for 8–9 days, the Tie2⁺ cells from E9.5 heads were significantly expanded (Figure 1E), to an average of 4.1×10^5 cells per head region (from three independent experiments). Flow cytometry detected CD19⁺ (44.6%–68.6%) populations (Figure 1F). For one embryo equivalent (ee), the Tie2⁺ head cells gave rise to 2.34×10^5 CD19⁺ B cells, slightly lower than the CH ones (Figure 1G). For T lymphocyte differentiation, three or four passages on fresh OP9-DL1 feeders were required over 3–4 weeks. From day 13 onward, the head/OP9-DL1 cocultures generated a CD25⁺CD44⁻ population, with a stepwise increase from 8.9% to 24.9%, indicating an early commitment to T cell lineage (Figure 1H). At day 26, the CD4⁺CD8⁺ and CD3⁺TCRβ⁺ populations reached up to 7.6% and 7.8%, respectively. That is, 1 ee of head could yield 1.13×10^9 CD4⁺CD8⁺ and 1.16×10^9 CD3⁺TCRβ⁺ cells in the coculture. Similarly, the Tie2⁺ cells from E9.5 CH gave rise to 1.70×10^9 CD4⁺CD8⁺ and 2.22×10^9 CD3⁺TCRβ⁺ cells (Figure 1H).

Development of Adult-Repopulating HSCs in the Mouse Embryonic Head

Long-term transplantation is widely accepted as the most stringent and reliable assay for HSC activity. Previous literatures indicate that the adult-repopulating HSCs are rare in the mouse E10.5 conceptus (Gekas et al., 2005; Kumaravelu et al., 2002; Müller et al., 1994). Müller et al. revealed that the first adult-reconstituting HSC arose exclusively in the AGM region of E10.5 conceptus (34–41 sp), but its engraftment efficiency was low as only 3 out of 96 recipients in total were repopulated (Müller et al., 1994). Since the E9.5–E11.5 head region demonstrated robust multipotent lymphomyeloid potential in vitro, we wondered whether adult-repopulating HSCs developed concurrently in this site. Here, to improve the efficacy, we used more cells (1.7–2.5 ee per recipient) and a higher radiation dose rate (2.3 Gy per minute). The total cell numbers for transplantation at indicated time points are shown in Table S1 (available online). As shown in Table 1 and Figure 2A, none of the recipients transplanted with 1 ee of E10.5 (36–41 sp) AGM was repopulated with >10% chimerism after 16 weeks (n = 13, four independent experiments). Three recipients displayed <5.0% chimerism after 4 weeks, but the positive signals disappeared when retested 16 weeks posttransplantation (data not shown). In contrast, with 1.7–2.5 ee injection, 14–15 out of 39–40 recipients (13 independent experiments) were repopulated, with an average short-term chimerism of $27.5\% \pm 14.6\%$ (>4 weeks)

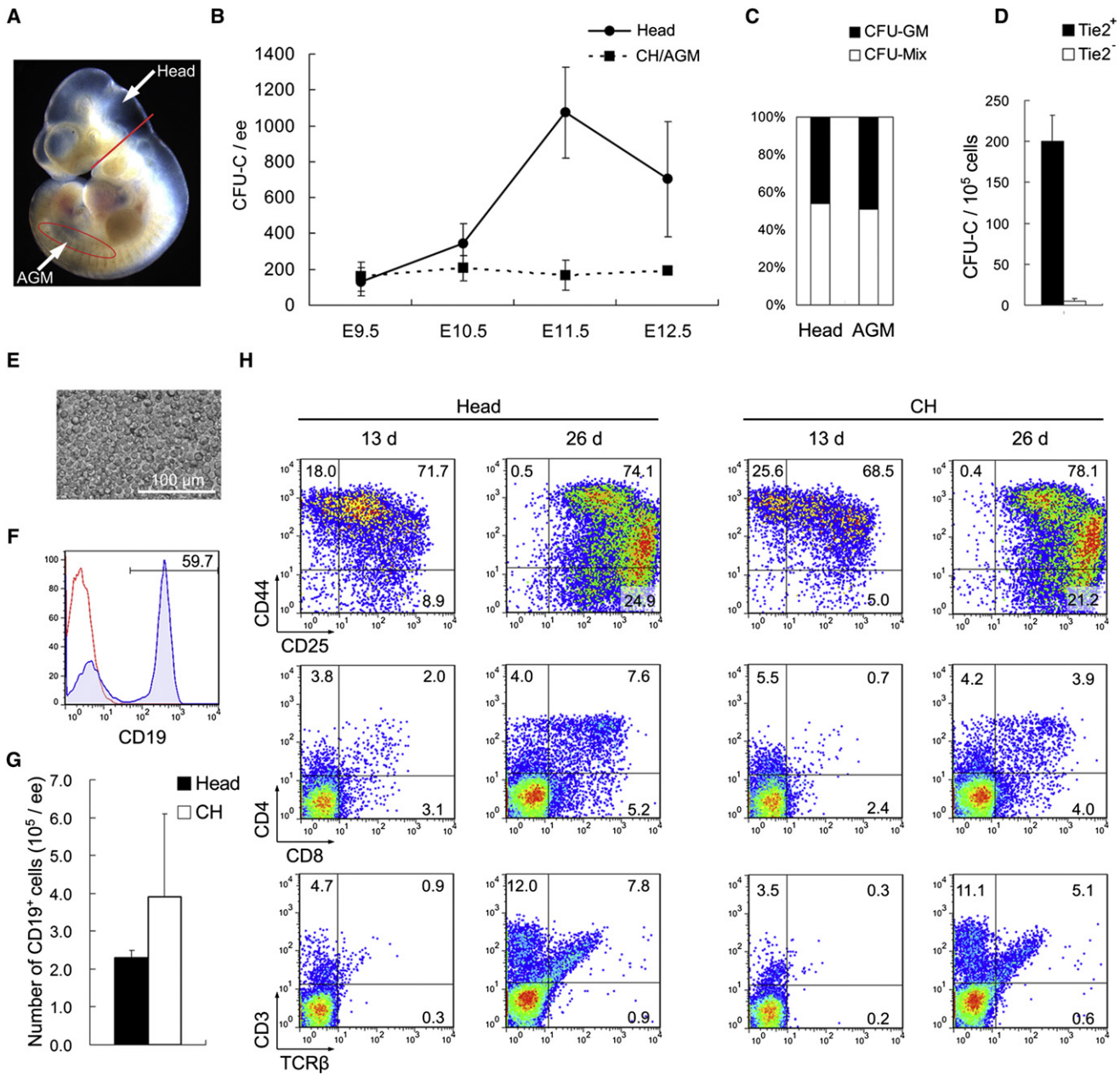


Figure 1. Lymphomyeloid Potential in the Mouse Embryonic Head

(A) Schematic dissection of head and AGM region from an E10.5 embryo.

(B) Numbers of CFU-Cs in E9.5–E12.5 head and caudal half (CH, E9.5) or AGM region (E10.5–E12.5). Data are expressed as means \pm SEM, and are collected from three (E9.5–E11.5) or two (E12.5) independent experiments.

(C) Percentage of CFU-GM and CFU-Mix in total CFU-Cs of head and AGM region at E10.5.

(D) Colony numbers per 10^5 cells were calculated in Tie2⁺ and Tie2⁻ populations of E10.5–E11.0 head. Data are means \pm SEM.

(E) Morphology of E9.5 head Tie2⁺ cells after 8–9 days of B lymphocyte induction on OP9, showing significant expansion of semiadherent population.

(F) Expression of CD19 in the E9.5 head cultures analyzed by flow cytometry.

(G) The absolute numbers of CD19⁺ cells per E9.5 tissue. Data are means \pm SEM from three independent experiments.

(H) T lymphoid potential in E9.5 head and CH. At indicated time points, expression of CD44/CD25, CD4/CD8, and CD3/TCR β in head (left two columns) and CH (right two columns) cocultured with OP9-DL1 were analyzed by flow cytometry.

and long-term chimerism of $46.6\% \pm 22.4\%$ (>16 weeks). In parallel, transplantation with E10.5 head cells led to successful reconstitution in 4–5 out of 40 recipients, with an average short-term chimerism of $27.3\% \pm 10.3\%$ and long-term chime-

rism of $57.2\% \pm 22.9\%$. Two successful recipients received donor cells from the heads of <40 sp (1 of 37–38 sp and 1 of 38–39 sp heads, from two independent experiments). However, transplantation with 1.7–2.5 ee cells from E10.5 embryonic

Table 1. The Emergence of Adult-Repopulating HSCs in the Mouse Embryonic Head and AGM Region

Time Posttransplantation				>4 Weeks		>16 Weeks	
Stage	Organ	ee ^a	Exp (n)	Re ^b /Total	Chimerism (%)	Re/Total	Chimerism (%)
E10.5 (36–41 sp ^c)	head	1	4	0/11	NA ^d	0/9	NA
		1.7–2.5	13	4/40	27.3 ± 10.3	5/40	57.2 ± 22.9
	AGM	1	4	0/13	NA	0/11	NA
		1.7–2.5	13	14/40	27.5 ± 14.6	15/39	46.6 ± 22.4
	blood	1	4	0/5	NA	0/5	NA
		1.7–2.5	11	0/29	NA	0/27	NA
E11.5 (42–50 sp)	head	0.3	4	1/16	48.0	2/23	19.5, 56.4
		1	6	10/18	27.8 ± 10.5	8/20	54.6 ± 23.8
	AGM	0.3	3	0/16	NA	0/16	NA
		1	5	9/15	32.8 ± 14.7	9/15	47.9 ± 20.9
	blood	0.3	1	0/5	NA	0/5	NA
		1	5	3/15	36.5 ± 6.5	3/15	48.0 ± 19.3
E12.5	head	0.5	3	12/21	39.5 ± 17.5	13/21	49.3 ± 19.0
	AGM	0.5	3	6/11	34.7 ± 14.2	5/11	50.1 ± 22.2

^aee, embryo equivalents.

^bRe, repopulated.

^csp, somite pairs.

^dNA, not available.

circulation (36–41 sp) did not repopulate the recipients (n = 29, 11 independent experiments), consistent with previous studies (Gekas et al., 2005; Müller et al., 1994). At E11.5, transplantation of 1 ee of head cells (42–50 sp) resulted in 40% of recipients (8/20) being efficiently repopulated, with an average long-term chimerism of 54.6% ± 23.8%. The efficiency was approaching that of the AGM region (60%, 9/15). Notably, two recipients could be repopulated with 0.3 ee of E11.5 head cells. At this time point, the embryonic circulating cells began to display reconstitution capacity (3 repopulated out of 15 recipients). Of note, repopulation was only detected in the recipients transplanted with late E11.5 circulating cells (from pooled 44–47 sp or 47–50 sp embryos). The inability of early E11.5 (<45 sp) embryonic circulating cells to reconstitute the adult hosts at high levels has been documented in several reports (Gekas et al., 2005; Müller et al., 1994). Furthermore, with infusion of 0.5 ee of E12.5 head cells, 13 out of 21 recipients could be efficiently repopulated, resembling that of the AGM region (5/11).

Bona fide HSCs are functionally identified by two features: multilineage reconstitution and self-renewal ability. We analyzed multilineage repopulation in hematopoietic organs from recipients of head or AGM-derived cells (Figures 2B–2E; Figures S1A–S1D). The presence of E10.5 head- (38–39 sp) derived GFP⁺ myeloid (Gr-1⁺ or Mac-1⁺), B lymphoid (B220⁺), and T lymphoid (CD3⁺) cells was detected in the peripheral blood of repopulated recipient 6 months after transplantation (Figure 2B). Likewise, in the BM, thymus, and spleen of the same recipient, efficient multilineage engraftment was observed (Figures 2C–2E). Furthermore, self-renewal capacity was investigated by secondary transplantation of 3 × 10⁶ BM cells from primary recipients that had been successfully repopulated with E10.5 head- or AGM-derived cells (Figure 2F). For instance, the BM cells from the recipient repopulated by head cells of 38–39 sp could efficiently engraft into the secondary hosts (H1

in Figure 2F), as revealed by multilineage chimerism in the peripheral blood 6 months after transplantation (Figure S1E). As expected, BM cells from E10.5 AGM-repopulated recipients (all donors of 36–41 sp) demonstrated a similar self-renewing capacity (Figure 2F and Figure S1E).

Subsequently, we analyzed the immunophenotype of head HSCs. Similar to CFU-Cs *in vitro*, transplantation of Tie2⁺ rather than Tie2⁻ population from E12.5 head led to reconstitution in 4 out of 12 recipients, similar to the AGM region (5/12, Figure 2G). Reportedly, HSCs in the mouse AGM, YS, and placenta reside in the CD34⁺c-Kit⁺ population (Gekas et al., 2005; Sánchez et al., 1996; Yoder et al., 1997). Likewise, the CD34⁺c-Kit⁺ population in the E12.5 head, constituting 0.2%–0.3% of collagenase-digested cells, could efficiently repopulate irradiated adult recipients (3/13) over 6 months (Figure S1F, two independent experiments).

Expression of Hematopoietic Genes in the Mouse Embryonic Head

Combinations of c-Kit with CD34, CD41, or CD45 were used to roughly calculate the number of hematopoietic precursors. The frequencies of CD34⁺c-Kit⁺, CD41⁺c-Kit⁺, and CD45⁺c-Kit⁺ cells were comparable between the head and AGM region of E10.5 embryos (Figure 3A). Quantitatively, 1 ee of E10.5 head contained 6.8 × 10³ CD34⁺c-Kit⁺, 4.0 × 10³ CD41⁺c-Kit⁺, and 3.8 × 10³ CD45⁺c-Kit⁺ cells on average (Figure 3B, three independent experiments). The double positive populations were also evident in the E9.5 and E11.5 head region (Figures S2A and S2B).

Next, real-time PCR was used to quantify the mRNA levels of hematopoietic/endothelial-related molecules in the head and AGM region. In particular, it is reported that Runx1 is expressed in all of the adult-repopulating HSCs of midgestation mouse embryos (North et al., 2002), and the proximal P2 promoter

(P2-Runx1) is more critically required, compared with the distal promoter, in the endothelium-hematopoietic cell transition (Bee et al., 2010; Chen et al., 2009; Sroczyńska et al., 2009). As shown in Figure 3C, at E10.5, the transcription levels of *Scl*, P2-Runx1, and GATA-2 in the head were 1.5-, 1.6-, and 2.3-fold relative, respectively, to that in the AGM region of littermates (three or four independent experiments). The expression levels of endothelial markers were comparable. Furthermore, the expression levels of three transcriptional factors were analyzed in specific subpopulations (Tie2⁺ or CD31⁺c-Kit⁺) that enriched hematopoietic potential in vitro and in vivo. Compared with E10.5, a significant decrease of P2-Runx1 transcription was observed in the CD31⁺c-Kit⁺ subsets of E11.5 embryos (Figure S2C), implying the downregulation of endothelial-hematopoietic transition. In contrast, a doubling of GATA-2 transcription at E11.5 might indicate expansion of hematopoietic stem progenitor cells (Figure S2C). Comparable expression of P2-Runx1 between head and AGM was observed in either Tie2⁺ or CD31⁺c-Kit⁺ population (Figures 3D and 3E). These data suggested a cellular and molecular phenotype matching the hematopoietic potential of the head.

Hematopoietic Potential and Phenotype in the Mouse E8.25 Head

A previous report has documented the hematopoietic potential of gastrulating head region in optimized conditions (Kanatsu and Nishikawa, 1996). Here, the head and CH were carefully isolated from the precirculation embryo proper (E8.25, 1–6 sp) (Figure S2D), digested into single-cell suspension, and transferred to OP9 stromal cells in accordance with recent reports (Yoshimoto et al., 2011). After 3 days, the clones composed of semiadherent round cells formed (Figure S2E), some of which underwent significant expansion within the next 5–7 days. As a result, the CH cells yielded a total of 83 clones in 11 experiments, and the head, 12 clones in 5 experiments. Flow cytometry analysis showed the presence of CD19⁺ cells in four experiments of the CH cocultures, a rate more frequent than that of the head cocultures (one experiment, Figure S2F). Notably, under the same conditions, the E8.25 YS was also capable of generating CD19⁺ B lymphocytes (data not shown). Subsequently, the cells coexpressing CD41 and c-Kit, which represent definitive hematopoietic progenitors (Ferkowicz et al., 2003; Mikkola et al., 2003), were analyzed by flow cytometry. As shown in Figure S2G, the head region and CH had 0.14%–0.44% and 0.11%–0.76% of CD41⁺c-Kit⁺ cells, respectively. At E8.5 (8–12 sp), the frequency was significantly increased in the head (1.24% on average) and CH (1.37% on average) (Figure S2G, three independent experiments). It was interesting to note that a small population of CD34⁺c-Kit⁺ was present in both E8.25 head and CH (Figure S2H). In comparison, expression of CD144, Sca-1, and CD45 was very limited in the c-Kit⁺ population (Figure S2H). Real-time PCR analysis showed comparable expression of *Scl*, *Flk-1*, and P2-Runx1 in the E8.25 head, compared with CH (Figure S2I).

Hemogenic Potential in the Mouse Embryonic Head

Given the obvious hematopoietic capacity of the embryonic head, we aimed to determine whether the head could generate blood cells de novo via an endothelial intermediate, which has

been observed in the known hemogenic sites, such as AGM, YS, and placenta. To address the issue, a set of experiments were conducted.

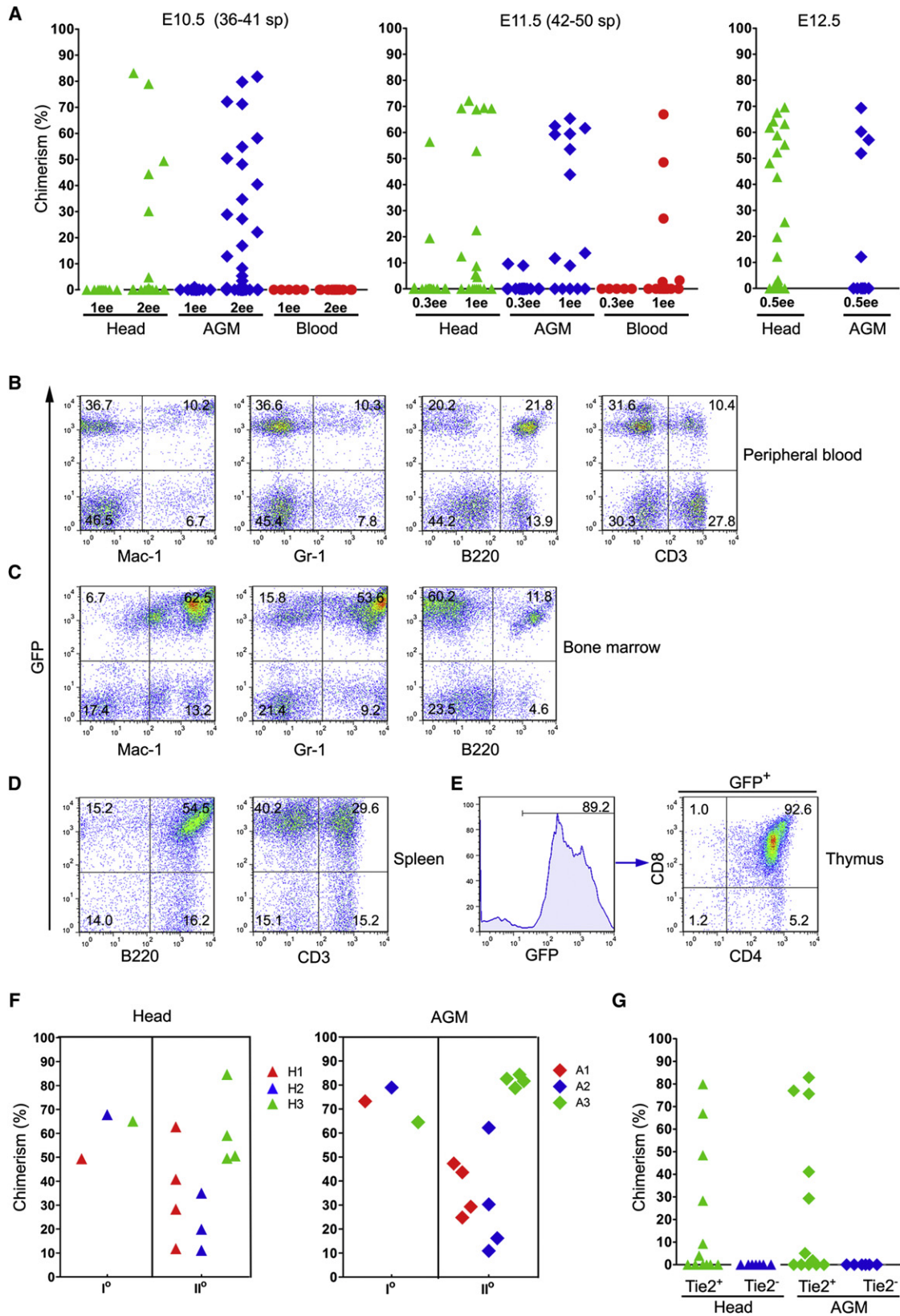
In the AGM region, intra-aortic cluster cells expressing endothelial markers are thought to grow out from the putative hemogenic endothelium, which is visualized initially at E9.5 and maximally at E10.5. Such cluster cells coincide with a distinguished CD31⁺c-Kit^{high} subset in flow cytometry (Yokomizo and Dzierzak, 2010). As shown in Figure 4A, the close association of the CD31⁺ cluster cells with the arterial endothelium was observed in the E10.5 head region. More importantly, as shown in Figure 4B, the E10.5 head had a unique CD31⁺c-Kit^{high} population (0.063%–0.113%, *n* = 3), resembling the AGM region (0.088%–0.157%, *n* = 3).

Next, to determine the existence of functional hemogenic endothelium, the assumptive endothelial cells, defined as CD31⁺CD41[−]CD45[−]Ter119[−] (Bee et al., 2010), in the E10.0 (31–36 sp) head were sorted by FACS and plated on the OP9 stromal cells (Figure 4C). After 2–3 days of culture, typical hemogenic clones appeared (Figure 4D), similar to those from AGM region. After 7–9 days, a considerable number of CD45⁺ hematopoietic cells and CD19⁺ B lymphocytes were detected (Figure 4E).

Recently, an in vitro noninvasive endothelial fate tracing strategy has been proven powerful and sensitive in distinguishing hemogenic from nonhemogenic organs (Zovein et al., 2008). As depicted in Figure 4F, the tamoxifen-inducible *VE-cadherin-Cre* line (Zovein et al., 2008) was crossed to the *ROSA-tdTOMATO* reporter line (Madisen et al., 2010). Then, the Tie2⁺ cells from head, AGM region, and circulating blood of the E11.0 double transgenic embryos were pulsed by 4-OHT for 24 hr and cocultured with OP9 stromal cells for an additional 4 days. Cre recombinase-induced expression of tdTOMATO in endothelial structures and hematopoietic clusters could be directly observed under microscope. The tdTOMATO⁺CD45[−] endothelial tubules were found in the groups of both head and AGM region, but not circulation (Figure 4G). As expected, in vitro 4-OHT induction did not label hematopoietic clusters generated from circulating cells (Figure 4H), consistent with previous reports (Zovein et al., 2008). In contrast, several hematopoietic clusters derived from the head became tdTOMATO⁺ and were positive for CD45, resembling those from the AGM region (Figure 4H). Flow cytometry further confirmed the presence of CD45⁺ hematopoietic cells in tdTOMATO⁺ population of both the head and AGM cultures and the lack of tdTOMATO⁺ population in the circulating blood cultures (Figure 4I). These data collectively verified that the embryonic head had hemogenic potential.

Physiological Contribution of Cerebrovascular-Specific Endothelial Cells to Embryonic and Postnatal Hematopoietic System

Recently, we developed a unique *SP-A-Cre* transgenic mouse line in which Cre activity in endothelial cells is restricted to the brain vasculature from E11.5 (Li et al., 2011; Meng et al., 2007). Conceivably, this model is optimal for tracing the hematopoietic fate of cerebrovascular endothelial cells. First, LacZ staining was performed in E12.5 *SP-A-Cre;ROSA-LacZ* double transgenic embryos. No LacZ⁺ cells were detected in the aortic endothelium



or in the fetal liver (Figure S3A). In comparison, simultaneous head sections showed that in some of the morphologically defined arterioles and arteries, blue-stained LacZ⁺ blood cells were detected and some appeared to be “budding” from the endothelial layer (Figure 5A). In contrast, no positive signal was observed in blood cells in the lumen of typical veins (Figure 5A). These data highly suggested an in situ hematopoietic activity in the cerebrovasculature.

Next, certain hematopoietic and endothelial populations were quantified by flow cytometry using fluorescein di-β-D-galactopyranoside (FDG) as the substrate for β-galactosidase (β-gal). The *Tie2-Cre* transgenic mice were examined in parallel as a positive control. The Tie2-Cre-mediated ablation occurs in all endothelial/hematopoietic cells from E8.5 (Lan et al., 2007), which is much earlier than SP-A-Cre expression, and encompasses the entire period of hemogenic activity in the endothelium. We demonstrated that in the head of E11.5 *Tie2-Cre;ROSA-LacZ* double transgenic mice, 48.1% of the CD31⁺ population and 45.4% of the CD45⁺ population were positive for β-gal expression. Moreover, 10.5% of the CD31⁺ population and 4.6% of the CD45⁺ population contained the recombinant allele in the head of E13.5 *SP-A-Cre;ROSA-LacZ* double transgenic mice (Figure 5B).

We then turned to an in vitro coculture system and found that after coculture with OP9, the Cre-mediated recombination in endothelial/hematopoietic cells derived from E12.5 head was greater than that in vivo. Tie2-Cre-mediated ablation was evidenced by a remarkable shift of the cell population peak to FDG⁺. In *SP-A-Cre;ROSA-LacZ* double transgenic mice, 20% of the CD31⁺ population and 8.4% of the CD45⁺ population were positive for FDG. When gated on the CD45⁺c-Kit⁺ population, representative of hematopoietic progenitors, 12.3% of cells were FDG⁺. Notably, when gated on the B220⁺CD19⁺ lymphocyte population, the hallmark of definitive hematopoiesis, 27.6% of cells were positive for expression of β-gal (Figure 5C). In contrast, FDG⁺CD45⁺ cells were not detected in the parallel culture of AGM cells from *SP-A-Cre;ROSA-LacZ* double transgenic mice (Figure S3B).

Finally, the physiological contribution of SP-A-expressing cells to the postnatal hematopoietic system was investigated. In the BM of 4-week-old *SP-A-Cre;ROSA-LacZ* double transgenic mice, approximately 4.2%–4.5% of the enriched HSC population (CD150⁺CD48⁻Lin⁻Sca-1⁺c-Kit⁺, CD150⁺CD48⁻LSK) (Kiel et al., 2005) exhibited β-gal labeling (Figure 6A). Multilineage contribution was also detected in the BM (Figure S4). In a simpler way, we used the *ROSA-EYFP* reporter mice to bypass the step

of FDG labeling (Srinivas et al., 2001). In the 4- to 6-week old *SP-A-Cre;ROSA-EYFP* double transgenic mice, EYFP⁺ cells constituted 5.9%–7.7% of the BM CD150⁺CD48⁻LSK population (Figures 6B and 6E). Moreover, different levels of contribution were detected in the erythroid (Ter119⁺, 2.3%–5.8%), myeloid (Gr-1⁺/Mac-1⁺, 3.1%–7.6%), B lymphoid (B220⁺, 1.8%–7.7%), and T lymphoid (CD3⁺, 2.8%–9.6%) cells of BM (Figures 6C and 6E). A similar pattern was present in the peripheral blood (Figures 6D and 6E).

DISCUSSION

In a conventional view, early intraembryonic hematopoiesis occurs exclusively in the caudal AGM region. Our findings provide evidence that the area of hematopoietic potential in the embryo proper may be larger than previously thought. As the earliest intraembryonic vasculogenesis occurs in the head region, our studies further emphasize the well-known developmental intimacy between vasculature and blood ontogeny.

In this study, the intraembryonic distribution of adult-type HSCs in midgestation mouse embryos was reevaluated using a modified irradiation strategy. Theoretically, an increased dose rate of irradiation can be more effective at depleting HSCs in the recipients and may induce greater production of various hematopoietic growth factors and cytokines. All these features can enhance donor cell engraftment. Unexpectedly, the early emergence of standard adult-repopulating HSCs was revealed in the E10.5–E12.5 head region. This finding may convincingly explain why E11 mouse embryo proper without AGM and fetal liver could successfully repopulate irradiated recipients (Müller et al., 1994). Intriguingly, at E10.5–E11.5, the donor chimerism by transplantation of head cells was very similar to that of AGM region, much higher than the E11.5–E12.5 fetal liver (Gekas et al., 2005). Nevertheless, the magnitude of HSC potential in the head, AGM, and YS is not as remarkable as that of the placenta, which harbors a large pool of approximately 50 adult-type HSCs at E12.5 (Gekas et al., 2005). Moreover, the head HSCs had a CD34⁺c-Kit⁺ and Tie2⁺ surface phenotype, similar to HSCs from AGM region, placenta, and YS. In contrast, the E12.5 fetal liver harbors both CD34⁺c-Kit⁺ and CD34⁻c-Kit⁺ HSCs (Gekas et al., 2005). In terms of HSC potential and phenotype, the head is more similar to the AGM region than the fetal liver.

Importantly, the head HSCs emerged before they could be detected in the embryonic circulation. Although considered to be responsible for HSC migration and exchange among distinct

Figure 2. Early Emergence of Adult-Repopulating HSCs in the Mouse Embryonic Head

(A) Repopulating potential of mouse embryonic head and AGM region at E10.5 (left), E11.5 (middle), and E12.5 (right). Symbols represent the donor chimerism of CD45⁺ cells in peripheral blood of individual recipients over 4 months posttransplantation. Injected dosage is expressed as embryo equivalents (ee) of hematopoietic tissues and circulating blood.

(B–E) Multilineage repopulation of E10.5 head cells after transplantation. The donor contribution is revealed by presence of GFP⁺ cells in the myeloid (Mac-1 and Gr-1), B lymphoid (B220), and T lymphoid (CD3, CD4, and CD8) cells of peripheral blood (B), BM (C), spleen (D), and thymus (E) of a representative recipient at 6 months posttransplantation. The recipient was injected with 2 ee of E10.5 head cells (38–39 sp).

(F) Repopulating potential of BM cells derived from repopulated primary recipients transplanted with E10.5 head (H1: 38–39 sp; H2 and H3: 36–41 sp) and AGM region (A1–A3: 36–41 sp). Symbols represent the donor chimerism of CD45⁺ cells in peripheral blood of individual secondary recipients over 6 months posttransplantation. Identical symbols indicate each donor and related secondary recipients.

(G) Immunophenotype of E12.5 head HSCs. Repopulating potential of Tie2⁺ and Tie2⁻ cells derived from E12.5 mouse embryonic head and AGM region (two independent experiments). Symbols represent the donor chimerism of CD45⁺ cells in peripheral blood of individual recipients over 4 months posttransplantation. See also Figure S1.

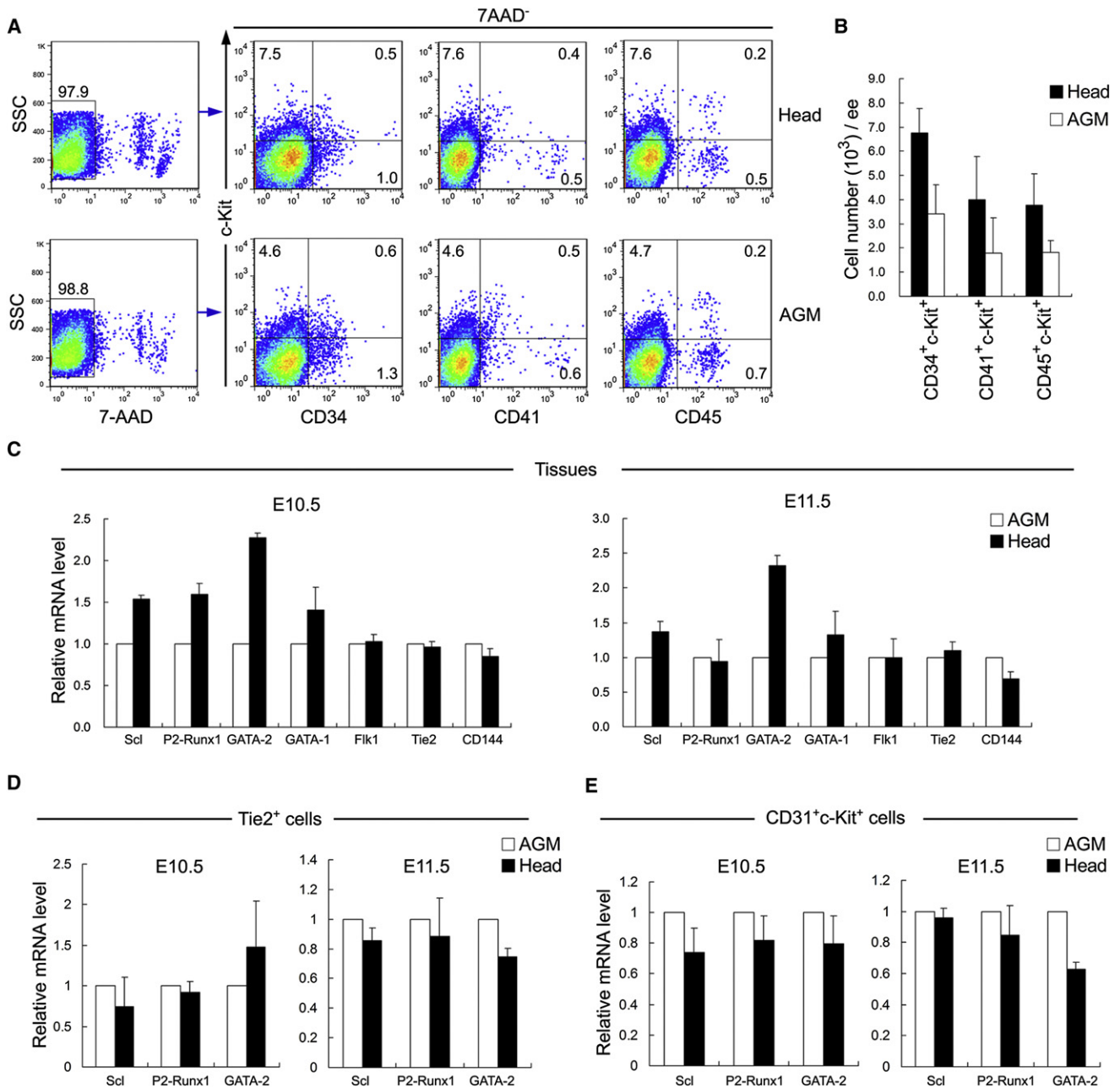


Figure 3. Cellular and Molecular Characterization of Hematopoietic Phenotype in the Mouse Embryonic Head

(A) Coexpression of c-Kit with CD34, CD41, or CD45 was analyzed in 7-AAD⁻ live cells of E10.5 head and AGM region by flow cytometry. Representative plots are shown.

(B) Quantification of CD34⁺c-Kit⁺, CD41⁺c-Kit⁺, and CD45⁺c-Kit⁺ cells in E10.5 head and AGM region. Data are means ± SEM from three independent experiments.

(C–E) Expression of hematopoietic-related transcriptional factors or/and endothelial molecules in the tissues (C), Tie2⁺ cells (D), or CD31⁺c-Kit⁺ cells (E) of E10.5–E11.5 head relative to AGM region analyzed by real-time PCR. Data are means ± SEM.

See also Figure S2.

anatomical sites, a precise timing of initial presence of HSCs in circulation has not been consensually validated. Here, we found that circulating cells in late E11.5 embryos were capable of reconstituting adult primary recipients. Surprisingly, the BM cells from two repopulated recipients failed to establish >5% chimerism in secondary recipients (data not shown). Previously, no

or low-level chimerism (<5%) has been observed in the peripheral blood of recipients infused with E11.5 circulating cells (Gekas et al., 2005; Müller et al., 1994; Yokomizo and Dzierzak, 2010). In contrast, Kumaravelu et al. conclude that E11.5 circulation contains HSCs; however, some key data, particularly those of the secondary transplantation, were not fully displayed

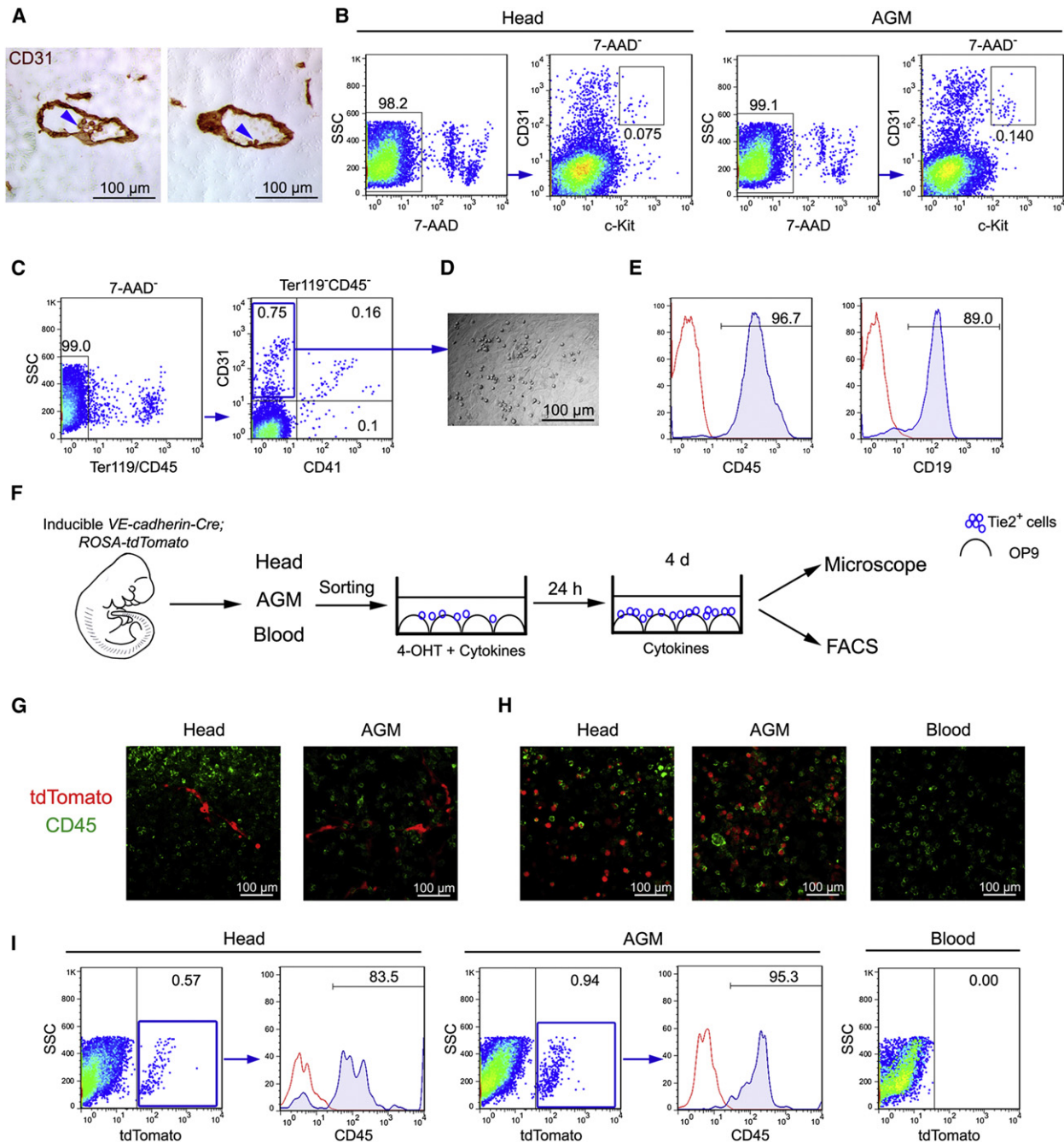


Figure 4. Hemogenic Potential in the Mouse Embryonic Head

(A) CD31 immunostaining (brown) of E10.5 head sections. Blue arrowheads indicate typical intraluminal cluster cells expressing CD31 “budding” from the endothelial layer of the vessel wall.

(B) Flow cytometry analysis reveals CD31⁺c-Kit^{high} cluster-like population in the 7-AAD⁻ live cells of head and AGM region of E10.5 embryos.

(C–E) Hemogenic potential of immunophenotypically defined endothelial cells in the head. Live endothelial cells (7-AAD⁻CD31⁺CD41⁻CD45⁻Ter119⁻) of E10.0 (31–36 sp) head were sorted by flow cytometry (C). Morphology of typical hemogenic clones after 2–3 days of OP9 coculture (D). Flow cytometry analysis detected CD45⁺ hematopoietic cells and CD19⁺ B lymphocytes after 7–9 days of coculture (E).

(F) Schematic illustration of the experimental protocol to explore the hemogenic potential in the head by using an inducible *VE-cadherin-Cre*;*ROSA-tdTomato* double transgenic mouse model.

(G and H) Fluorescence microscope examination of CD45 immunostained cultures, showing the *VE-cadherin-Cre* recombinase-induced expression of tdTOMATO (red) in endothelial tubules in the cultures of head and AGM region (G), and tdTOMATO⁺ (red) CD45⁺ (green) hematopoietic cells in the cultures of head and AGM region, contrasting with only tdTOMATO⁻CD45⁺ cells in the culture of circulating blood (H).

(I) Flow cytometry analysis shows CD45 expression in gated tdTOMATO⁺ populations from both head and AGM cultures and lack of tdTOMATO⁺ population in the circulating blood culture.

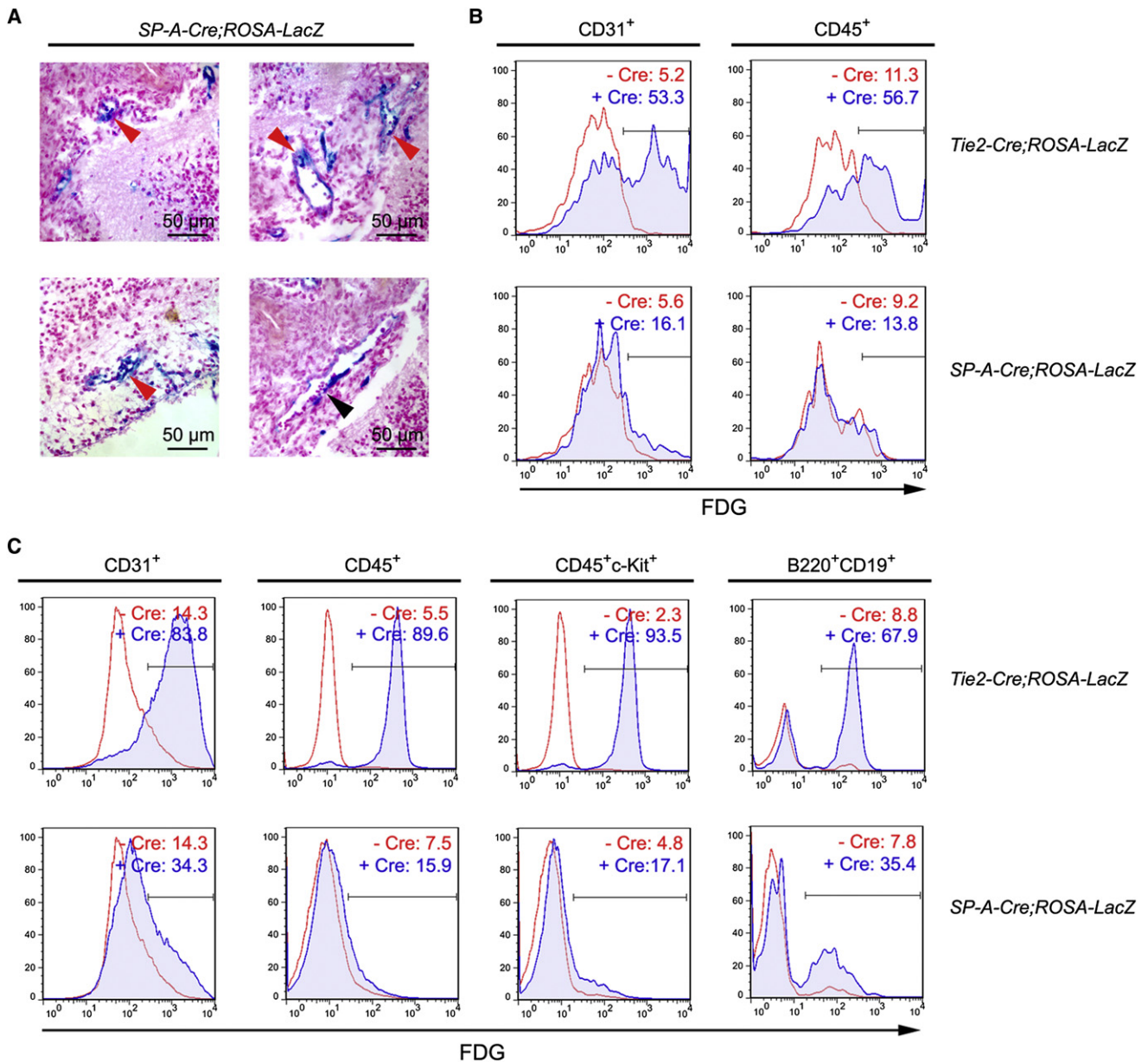


Figure 5. Hematopoietic Potential of Cerebrovascular Endothelial Cells in the Mouse Embryo

(A) Head sections of whole-mount LacZ-stained E12.5 *SP-A-Cre; ROSA-LacZ* double transgenic embryos, showing β -gal-labeled endothelial and blood cells. Red arrowheads show vessels with β -gal⁺ blood cells inside and some closely associated with the endothelial layer. Black arrowhead shows a vein without internal β -gal⁺ blood cells.

(B and C) FACS analysis of β -gal activity in the subpopulations of freshly prepared head cells from E11.5 *Tie2-Cre; ROSA-LacZ* (upper) and E13.5 *SP-A-Cre; ROSA-LacZ* (lower) double transgenic embryos (B), and of the cultured Tie2⁺ head cells from E12.5 *Tie2-Cre; ROSA-LacZ* (upper) and E12.5 *SP-A-Cre; ROSA-LacZ* (lower) double transgenic embryos (C). *ROSA-LacZ* littermates without the *Cre* transgene (–*Cre*) serve as negative controls (red lines). The *Cre*-mediated recombination is indicated by a shift of the cell population to FDG⁺.

See also Figure S3.

in the literature (Kumaravelu et al., 2002). The question of whether authentic HSCs appear in E11.5 embryonic circulation needs future examination.

We further delineated that, similar to the dorsal aorta, the embryonic head contained a specific type of endothelium that was hemogenic and harbored de novo blood-forming capacity. Here, three approaches were employed based on an in vitro

OP9 coculture system to reflect the hemogenic potential of head endothelium, two of which involved *Cre*-mediated fate tracing of temporally or spatially confined endothelial cells. The advantage of the inducible *VE-cadherin-Cre* line is that it can delicately recognize the true hemogenic sites via separate organ cultures (Zovein et al., 2008). In contrast to the AGM and the head region, hemogenic potential was absent in circulation,

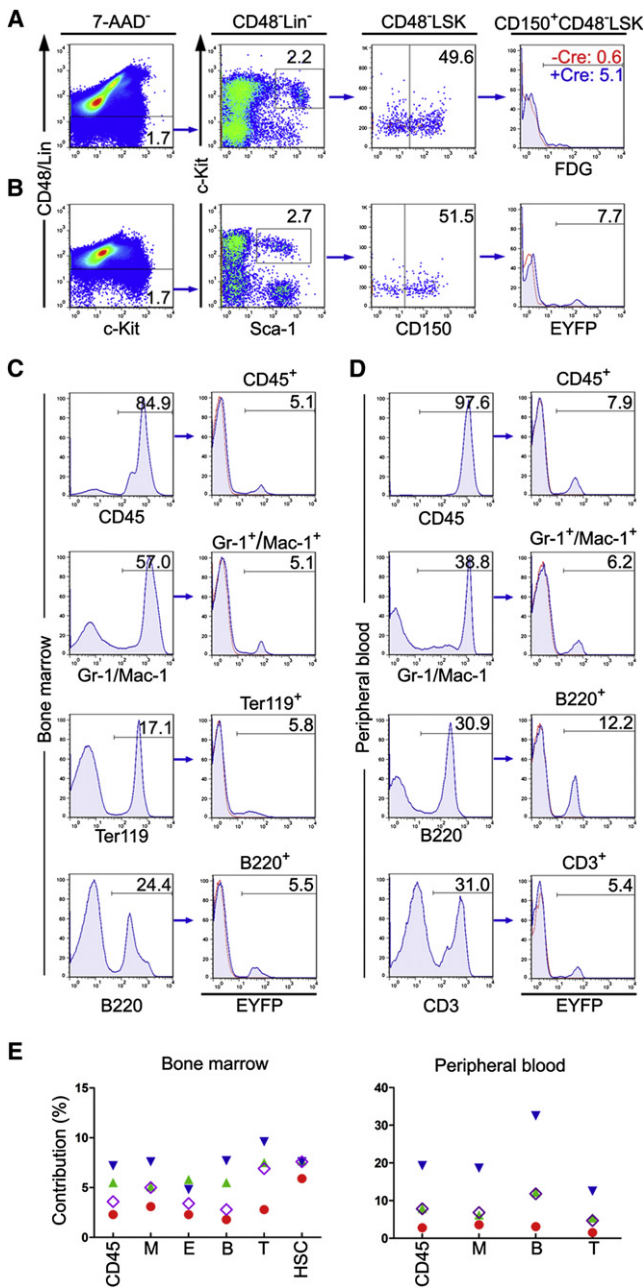


Figure 6. Contribution of Cerebrovascular Endothelial Cells to Postnatal Hematopoietic System

(A) Representative FACS analysis of β -gal activity in the putative HSCs ($CD150^+CD48^-LSK$) of $7-AAD^-$ live BM cells from a 4-week-old *SP-A-Cre; ROSA-LacZ* double transgenic mouse. The *ROSA-LacZ* littermate without the *Cre* transgene (-Cre) serves as negative control (red lines). The *Cre*-mediated recombination is indicated by the shift of the cell population to FDG^+ .

(B–D) Representative FACS analysis of EYFP fluorescence in $CD150^+CD48^-LSK$ of BM cells (B) and in multilineages of BM (C) and peripheral blood (D) from a 6-week-old *SP-A-Cre; ROSA-EYFP* double transgenic mouse. The *ROSA-EYFP* littermate without the *Cre* transgene serves as negative control (red lines).

(E) Percentage of EYFP⁺ cells in the BM and peripheral blood of 4- to 6-week-old *SP-A-Cre; ROSA-EYFP* double transgenic mice. M: myeloid lineage, Gr-1⁺/Mac-1⁺; E: erythroid lineage, Ter119⁺; B: B lymphoid lineage,

suggesting that the considerable circulation-derived hematopoiesis on OP9 must be a result of hematopoietic expansion rather than hemogenesis from the endothelium. Therefore, the head is now identified as a member of the group of specific vascular beds for HSC emergence. In the near future, the technology of real-time imaging of the AGM region should be refined and used to directly witness de novo generation of phenotypically and even functionally defined hematopoietic stem progenitor cells from the cerebrovasculature (Boisset et al., 2011).

Among the strategies used to define the spatial origin of adult HSCs, lineage tracing via specific *Cre* transgenes has provided the most physiological evidence (Samokhvalov et al., 2007; Yoshimoto et al., 2008; Zovein et al., 2008). The *SP-A-Cre* transgenic mouse is a valuable and unique tool to investigate hematopoietic potential exclusively in the head. Importantly, the observation that hematopoietic activity in *SP-A-Cre*-expressing cells and their progeny was detected only in the head and not in other tissues of midgestation embryos strongly indicated the in situ emergence of blood cells. As documented, via a putative endothelial-hematopoietic transition, all HSCs became $CD45^+$ in the E11.5 AGM region (Kumaravelu et al., 2002; North et al., 2002), the time when *SP-A-Cre* began to be expressed in the embryonic head. It is conceivable that the hemogenic activity of endothelium after E11.5 may be a remnant. Notably, the distinct endothelial populations derived from *SP-A-Cre*-expressing cells constituted only 10%–20% of $CD31^+$ endothelial cells in the developing embryonic head. Therefore, the contribution of the cerebrovasculature to postnatal blood cells may be underestimated in this system. Even so, a clear contribution of these endothelial cells to all the mature lineages and putative HSCs was detected in postnatal BM and peripheral blood. Therefore, this model enables us to discern, isolate, and analyze the postnatal blood cells of a precise embryonic origin.

Importantly, the emergence of hematopoietic precursor cells during head vasculature development may have certain clinical implications. For example, hemangioblastoma, which is a type of central nervous system tumor, is highly vascularized and occurs sporadically or as a component of von Hippel-Lindau (VHL) disease (an autosomal dominantly inherited disorder). The cytological origin of hemangioblastoma is not clear. Surprisingly, the neoplastic cells express Brachyury, Scl, Flk-1, Tie2, and GATA-1 and are able to form blood-island-like structures with hematopoietic potential (Gläscher et al., 2006; Vortmeyer et al., 2003). Given the in situ hematopoietic potential of cerebral endothelial cells described here, whether hemangioblastoma originates from developmentally arrested precursors in the embryonic head deserves further investigations.

EXPERIMENTAL PROCEDURES

Animals

Mice were kept at the Animal Center of the Academy of Military Medical Sciences according to institutional guidelines. *GFP*-transgenic mice, inducible *VE-cadherin-Cre* transgenic mice, *SP-A-Cre* transgenic mice, *Tie2-Cre* transgenic mice, *ROSA-LacZ* reporter mice, *ROSA-tdTOMATO* reporter mice, and *ROSA-EYFP* reporter mice have been reported elsewhere (Lan et al., 2007;

B220⁺; T: T lymphoid lineage, $CD3^+$; HSC: $CD150^+CD48^-LSK$. Identical symbols indicate related data from an individual (n = 4, from four litters). See also Figure S4.

Li et al., 2011; Madisen et al., 2010; Meng et al., 2007; Soriano, 1999; Srinivas et al., 2001; Tan et al., 2005; Zovein et al., 2008).

OP9 Cocultures

To determine hematopoietic or hemogenic potential, MACS-sorted Tie2⁺ cells or FACS-sorted CD31⁺CD41⁻CD45⁻Ter119⁻ endothelial cells were cultured on mouse OP9 stromal cells and supplemented with hematopoietic cytokines (50 ng/ml SCF, 10 ng/ml IL3, 10 ng/ml FL, 10 ng/ml IL-7, and 3 U/ml Epo) or angiogenic cytokine (100 ng/ml VEGF). For inducible *VE-cadherin-Cre;R-Osa-taTOMATO* embryos, the Tie2⁺ cells from head, AGM, and circulating blood were initially treated with 10 μ M of 4-OHT (Sigma). After being cultured for 5–10 days, cells were harvested by mechanical pipetting (hematopoietic cells) or digesting (endothelial cells) for flow cytometry analysis.

Transplantation Assay

Male GFP-transgenic mice on a C57BL/6 background and female C57BL/6 mice were used to obtain GFP⁺ embryos. With this strategy, contamination by maternal cells could be avoided. Female C57BL/6 mice were exposed to a split dose of 9 Gy γ -irradiation (⁶⁰Co) and injected via tail vein with GFP-transgenic cells from different tissues or embryonic blood. Simultaneous injection of 2 \times 10⁴ nucleated BM cells of C57BL/6 mice was used to promote short-term survival. Peripheral blood of the recipients was collected at the indicated time points. Greater than 10% GFP⁺ cells as determined by FACS was considered successful reconstitution. A total of 3 \times 10⁶ cells from the BM of reconstituted mice >4–6 months posttransplantation were injected into secondary recipients to examine self-renewal potential.

Flow Cytometry

Surface markers on enzymatically treated embryonic tissues, lymphocyte differentiation in vitro, and hematopoietic reconstitution in vivo were analyzed by flow cytometer FACS Calibur or Aria 2 (BD Biosciences). 7-amino-actinomycin D (7-AAD) was used to exclude dead cells. Data were analyzed with FlowJo software (Tree Star Inc., Ashland, OR). Flow cytometric measurement of β -gal activity was performed by using FDG (Sigma) in accordance with the manufacturer's instructions. Cells loaded with FDG were further stained with other antibodies using standard procedures.

Statistical Methods

Data were evaluated using a Student's two-tail t test. $p < 0.05$ was considered to be statistically significant.

SUPPLEMENTAL INFORMATION

Supplemental Information for this article includes four figures, one table, and Supplemental Experimental Procedures and can be found with this article online at <http://dx.doi.org/10.1016/j.stem.2012.07.004>.

ACKNOWLEDGMENTS

We thank Tao Cheng, Feng Ma, Sheng Zhou, Daohong Zhou, Yongchun Yu, Xiaobing Yuan, Tingxi Liu, Ting Zhou, and Jiabo Wang for helpful discussion. We thank M. Luisa Iruela-Arispe for kindly providing the inducible *VE-cadherin-Cre* mouse line. This work was supported by Chinese National Key Program on Basic Research (2011CB964800, 2012CB945100, 2012CB966904, and 2009CB941102) and National Natural Science Foundation of China (30911130360, 31030040, 81090410, 30871410, 30900570, 81071055, 31171416, and 31171410). The authors declare that they have no competing financial interests.

Received: September 27, 2011

Revised: April 25, 2012

Accepted: July 2, 2012

Published: November 1, 2012

REFERENCES

Bee, T., Swiers, G., Muroi, S., Pozner, A., Nottingham, W., Santos, A.C., Li, P.S., Taniuchi, I., and de Bruijn, M.F. (2010). Nonredundant roles for Runx1

alternative promoters reflect their activity at discrete stages of developmental hematopoiesis. *Blood* 115, 3042–3050.

Bennett, C.M., Kanki, J.P., Rhodes, J., Liu, T.X., Paw, B.H., Kieran, M.W., Langenau, D.M., Delahaye-Brown, A., Zon, L.I., Fleming, M.D., and Look, A.T. (2001). Myelopoiesis in the zebrafish, *Danio rerio*. *Blood* 98, 643–651.

Boisset, J.C., Andrieu-Soler, C., van Cappellen, W.A., Clapes, T., and Robin, C. (2011). Ex vivo time-lapse confocal imaging of the mouse embryo aorta. *Nat. Protoc.* 6, 1792–1805.

Chen, M.J., Yokomizo, T., Zeigler, B.M., Dzierzak, E., and Speck, N.A. (2009). Runx1 is required for the endothelial to haematopoietic cell transition but not thereafter. *Nature* 457, 887–891.

Cumano, A., and Godin, I. (2007). Ontogeny of the hematopoietic system. *Annu. Rev. Immunol.* 25, 745–785.

Cumano, A., Dieterlen-Lievre, F., and Godin, I. (1996). Lymphoid potential, probed before circulation in mouse, is restricted to caudal intraembryonic splanchnopleura. *Cell* 86, 907–916.

de Bruijn, M.F., Speck, N.A., Peeters, M.C., and Dzierzak, E. (2000). Definitive hematopoietic stem cells first develop within the major arterial regions of the mouse embryo. *EMBO J.* 19, 2465–2474.

Drake, C.J., and Fleming, P.A. (2000). Vasculogenesis in the day 6.5 to 9.5 mouse embryo. *Blood* 95, 1671–1679.

Dzierzak, E., and Speck, N.A. (2008). Of lineage and legacy: the development of mammalian hematopoietic stem cells. *Nat. Immunol.* 9, 129–136.

Ferkowicz, M.J., Starr, M., Xie, X., Li, W., Johnson, S.A., Shelley, W.C., Morrison, P.R., and Yoder, M.C. (2003). CD41 expression defines the onset of primitive and definitive hematopoiesis in the murine embryo. *Development* 130, 4393–4403.

Gekas, C., Dieterlen-Lievre, F., Orkin, S.H., and Mikkola, H.K. (2005). The placenta is a niche for hematopoietic stem cells. *Dev. Cell* 8, 365–375.

Gläsker, S., Li, J., Xia, J.B., Okamoto, H., Zeng, W., Lonser, R.R., Zhuang, Z., Oldfield, E.H., and Vortmeyer, A.O. (2006). Hemangioblastomas share protein expression with embryonal hemangioblast progenitor cell. *Cancer Res.* 66, 4167–4172.

Herbomel, P., Thisse, B., and Thisse, C. (1999). Ontogeny and behaviour of early macrophages in the zebrafish embryo. *Development* 126, 3735–3745.

Kanatsu, M., and Nishikawa, S.I. (1996). In vitro analysis of epiblast tissue potency for hematopoietic cell differentiation. *Development* 122, 823–830.

Kiel, M.J., Yilmaz, O.H., Iwashita, T., Yilmaz, O.H., Terhorst, C., and Morrison, S.J. (2005). SLAM family receptors distinguish hematopoietic stem and progenitor cells and reveal endothelial niches for stem cells. *Cell* 121, 1109–1121.

Kumaravelu, P., Hook, L., Morrison, A.M., Ure, J., Zhao, S., Zuyev, S., Ansell, J., and Medvinsky, A. (2002). Quantitative developmental anatomy of definitive haematopoietic stem cells/long-term repopulating units (HSC/RUS): role of the aorta-gonad-mesonephros (AGM) region and the yolk sac in colonisation of the mouse embryonic liver. *Development* 129, 4891–4899.

Lan, Y., Liu, B., Yao, H., Li, F., Weng, T., Yang, G., Li, W., Cheng, X., Mao, N., and Yang, X. (2007). Essential role of endothelial Smad4 in vascular remodeling and integrity. *Mol. Cell. Biol.* 27, 7683–7692.

Le Guyader, D., Redd, M.J., Colucci-Guyon, E., Murayama, E., Kissa, K., Briolat, V., Mordelet, E., Zapata, A., Shinomiya, H., and Herbomel, P. (2008). Origins and unconventional behavior of neutrophils in developing zebrafish. *Blood* 111, 132–141.

Li, F., Lan, Y., Wang, Y., Wang, J., Yang, G., Meng, F., Han, H., Meng, A., Wang, Y., and Yang, X. (2011). Endothelial Smad4 maintains cerebrovascular integrity by activating N-cadherin through cooperation with Notch. *Dev. Cell* 20, 291–302.

Lux, C.T., Yoshimoto, M., McGrath, K., Conway, S.J., Palis, J., and Yoder, M.C. (2008). All primitive and definitive hematopoietic progenitor cells emerging before E10 in the mouse embryo are products of the yolk sac. *Blood* 111, 3435–3438.

Madisen, L., Zwingman, T.A., Sunkin, S.M., Oh, S.W., Zariwala, H.A., Gu, H., Ng, L.L., Palmiter, R.D., Hawrylycz, M.J., Jones, A.R., et al. (2010). A robust

- and high-throughput Cre reporting and characterization system for the whole mouse brain. *Nat. Neurosci.* **13**, 133–140.
- McGrath, K.E., and Palis, J. (2005). Hematopoiesis in the yolk sac: more than meets the eye. *Exp. Hematol.* **33**, 1021–1028.
- Medvinsky, A., and Dzierzak, E. (1996). Definitive hematopoiesis is autonomously initiated by the AGM region. *Cell* **86**, 897–906.
- Meng, F., Shi, L., Cheng, X., Hou, N., Wang, Y., Teng, Y., Meng, A., and Yang, X. (2007). Surfactant protein A promoter directs the expression of Cre recombinase in brain microvascular endothelial cells of transgenic mice. *Matrix Biol.* **26**, 54–57.
- Mikkola, H.K., and Orkin, S.H. (2006). The journey of developing hematopoietic stem cells. *Development* **133**, 3733–3744.
- Mikkola, H.K., Fujiwara, Y., Schlaeger, T.M., Traver, D., and Orkin, S.H. (2003). Expression of CD41 marks the initiation of definitive hematopoiesis in the mouse embryo. *Blood* **101**, 508–516.
- Müller, A.M., Medvinsky, A., Strouboulis, J., Grosveld, F., and Dzierzak, E. (1994). Development of hematopoietic stem cell activity in the mouse embryo. *Immunity* **1**, 291–301.
- North, T.E., de Bruijn, M.F., Stacy, T., Talebian, L., Lind, E., Robin, C., Binder, M., Dzierzak, E., and Speck, N.A. (2002). Runx1 expression marks long-term repopulating hematopoietic stem cells in the midgestation mouse embryo. *Immunity* **16**, 661–672.
- Ottersbach, K., and Dzierzak, E. (2005). The murine placenta contains hematopoietic stem cells within the vascular labyrinth region. *Dev. Cell* **8**, 377–387.
- Palis, J., Robertson, S., Kennedy, M., Wall, C., and Keller, G. (1999). Development of erythroid and myeloid progenitors in the yolk sac and embryo proper of the mouse. *Development* **126**, 5073–5084.
- Rhodes, K.E., Gekas, C., Wang, Y., Lux, C.T., Francis, C.S., Chan, D.N., Conway, S., Orkin, S.H., Yoder, M.C., and Mikkola, H.K. (2008). The emergence of hematopoietic stem cells is initiated in the placental vasculature in the absence of circulation. *Cell Stem Cell* **2**, 252–263.
- Samokhvalov, I.M., Samokhvalova, N.I., and Nishikawa, S. (2007). Cell tracing shows the contribution of the yolk sac to adult haematopoiesis. *Nature* **446**, 1056–1061.
- Sánchez, M.J., Holmes, A., Miles, C., and Dzierzak, E. (1996). Characterization of the first definitive hematopoietic stem cells in the AGM and liver of the mouse embryo. *Immunity* **5**, 513–525.
- Soriano, P. (1999). Generalized lacZ expression with the ROSA26 Cre reporter strain. *Nat. Genet.* **21**, 70–71.
- Srinivas, S., Watanabe, T., Lin, C.S., William, C.M., Tanabe, Y., Jessell, T.M., and Costantini, F. (2001). Cre reporter strains produced by targeted insertion of EYFP and ECFP into the ROSA26 locus. *BMC Dev. Biol.* **1**, 4.
- Sroczyńska, P., Lancrin, C., Kouskoff, V., and Lacaud, G. (2009). The differential activities of Runx1 promoters define milestones during embryonic hematopoiesis. *Blood* **114**, 5279–5289.
- Tan, X.W., Liao, H., Sun, L., Okabe, M., Xiao, Z.C., and Dawe, G.S. (2005). Fetal microchimerism in the maternal mouse brain: a novel population of fetal progenitor or stem cells able to cross the blood-brain barrier? *Stem Cells* **23**, 1443–1452.
- Taoudi, S., Gonneau, C., Moore, K., Sheridan, J.M., Blackburn, C.C., Taylor, E., and Medvinsky, A. (2008). Extensive hematopoietic stem cell generation in the AGM region via maturation of VE-cadherin+CD45+ pre-definitive HSCs. *Cell Stem Cell* **3**, 99–108.
- Vortmeyer, A.O., Frank, S., Jeong, S.Y., Yuan, K., Ikejiri, B., Lee, Y.S., Bhowmick, D., Lonser, R.R., Smith, R., Rodgers, G., et al. (2003). Developmental arrest of angioblastic lineage initiates tumorigenesis in von Hippel-Lindau disease. *Cancer Res.* **63**, 7051–7055.
- Yoder, M.C., Hiatt, K., Dutt, P., Mukherjee, P., Bodine, D.M., and Orlic, D. (1997). Characterization of definitive lymphohematopoietic stem cells in the day 9 murine yolk sac. *Immunity* **7**, 335–344.
- Yokomizo, T., and Dzierzak, E. (2010). Three-dimensional cartography of hematopoietic clusters in the vasculature of whole mouse embryos. *Development* **137**, 3651–3661.
- Yoshimoto, M., Porayette, P., and Yoder, M.C. (2008). Overcoming obstacles in the search for the site of hematopoietic stem cell emergence. *Cell Stem Cell* **3**, 583–586.
- Yoshimoto, M., Montecino-Rodriguez, E., Ferkowicz, M.J., Porayette, P., Shelley, W.C., Conway, S.J., Dorshkind, K., and Yoder, M.C. (2011). Embryonic day 9 yolk sac and intra-embryonic hemogenic endothelium independently generate a B-1 and marginal zone progenitor lacking B-2 potential. *Proc. Natl. Acad. Sci. USA* **108**, 1468–1473.
- Zovein, A.C., Hofmann, J.J., Lynch, M., French, W.J., Turlo, K.A., Yang, Y., Becker, M.S., Zanetta, L., Dejana, E., Gasson, J.C., et al. (2008). Fate tracing reveals the endothelial origin of hematopoietic stem cells. *Cell Stem Cell* **3**, 625–636.